Investigation of V_2O_5/Nb_2O_5 Catalysts by ^{51}V Solid-State NMR

R. H. H. Smits, K. Seshan,* and J. R. H. Ross†

Faculty of Chemical Technology, University of Twente, P.O. Box 217, 7500 AE Enschede, The Netherlands

A. P. M. Kentgens*

NSR Center for Molecular Structure, Design and Synthesis, SON/NWO HF-NMR Facility, University of Nijmegen, Toernooiveld, 6525 ED Nijmegen, The Netherlands

Received: November 10, 1994; In Final Form: February 27, 1995⊗

Vanadium–niobium oxide catalysts containing variable amounts of vanadium and prepared by coprecipitation were investigated using ^{51}V solid-state NMR. It was found that, in samples containing less than about 8 mol % V_2O_5, vanadium occurs in three different oxygen environments: in isolated tetrahedra, in corner-sharing tetrahedra (pyrovanadate), and in distorted octahedra. The number of octahedral sites increased as the amount of vanadium in the bulk of the catalyst was increased. The compound β-$(Nb,V)_2O_5$ was found to occur in samples containing more than 7 mol % V_2O_5. In this compound, vanadium occurs not only in isolated tetrahedral sites but also in corner-sharing tetrahedral sites. For a catalyst having the niobia in the crystalline T form, it was found that an increase in the bulk concentration of vanadium caused the number of neighboring sites occupied by vanadium to increase and the vanadium partially to replace niobium in the T-niobia structure.

Introduction

Oxidative Dehydrogenation of Propane on Vanadium–Niobium Oxide Catalysts. Niobia-based systems are efficient catalysts for the selective oxidative conversion of lower alkanes. Catalytic oxidative dehydrogenation of alkanes (C_3, C_4) to the corresponding olefins is of current interest because of its advantages over conventional dehydrogenation.[1–3] The advantages include overcoming the problems involved in carrying out catalytic dehydrogenation such as equilibrium-limited conversions and easy coke formation which causes rapid catalyst deactivation.[4] A disadvantage of oxidative conversion is that maintaining high selectivity to olefins (as against combustion) at useful conversions is difficult. We have shown earlier that niobium pentoxide is a very selective catalyst for the oxidative conversion of propane to propylene[5,6] even though its catalytic activity was only moderate. Subsequently, we have shown that by promoting niobium pentoxide with elements such as vanadium, chromium, or molybdenum[7,8] the catalytic activity can be improved considerably while maintaining the high selectivity to propylene that unpromoted niobia showed. Among the three mentioned, vanadium was found to be the optimal promoter.[7,8] It was found that the method of addition of the vanadium to the niobium oxide had a large influence on the performance of the resulting catalyst;[9] a method such as coprecipitation was most beneficial because it gave a homogeneous distribution of the vanadium in the catalyst. It was shown, for catalysts containing 7 mol % V_2O_5 or less, that the rates of propane conversion per vanadium site increased more than linearly with the surface concentration of vanadium, indicating that there is a geometric requirement for the active site.[10] At bulk vanadium concentrations higher than 7 mol %, mixed vanadium–niobium oxides such as β-$(Nb,V)_2O_5$ were formed;[11] rates of propane conversion per vanadium site were lower when the mixed oxides occurred.[4,10]

Model. We propose a model to explain the results described above in order to identify the active sites in these catalysts. In the catalysts reported here niobia is mostly present as a monoclinic phase denoted T-Nb_2O_5.[11,12] As the amount of vanadium added homogeneously to the niobia is increased, the niobium in the crystal structure is replaced by vanadium. This vanadium may occupy the sites normally occupied by niobium ions in the T-Nb_2O_5. The activity of each vanadium site at the surface increases as more neighboring sites are occupied by vanadium; this increase is caused by the formation of V–O–V ensembles which have a more reactive bridging oxygen than do the V–O–Nb ensembles. (The former are easier to reduce than the latter as seen by temperature-programmed reduction[4,10].) This change in the number of vanadium and niobium species in the second coordination sphere around a vanadium site is shown in Figure 1. The lower activity of vanadium sites when present in the mixed phase (assumed to be in isolated tetrahedral sites[11,12]) may be due to the absence of V–O–V ensembles and their environment again being dominated by niobium ions.

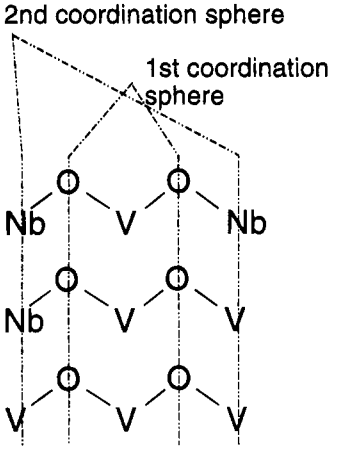

Figure 1. Formation of V–O–V ensembles and decrease of the number of niobium atoms in the second coordination sphere with increasing vanadium concentration. The broken lines are drawn to show the coordination spheres.

In order to verify this model experimentally, it was decided to study the local environment of the vanadium ions using ^{51}V solid-state NMR. This paper investigates the following

* To whom correspondence should be addressed.

† Present address: University of Limerick, Plassey Technological Park, Limerick, Ireland.

⊗ Abstract published in *Advance ACS Abstracts,* May 1, 1995.

0022-3654/95/2099-9169$09.00/0

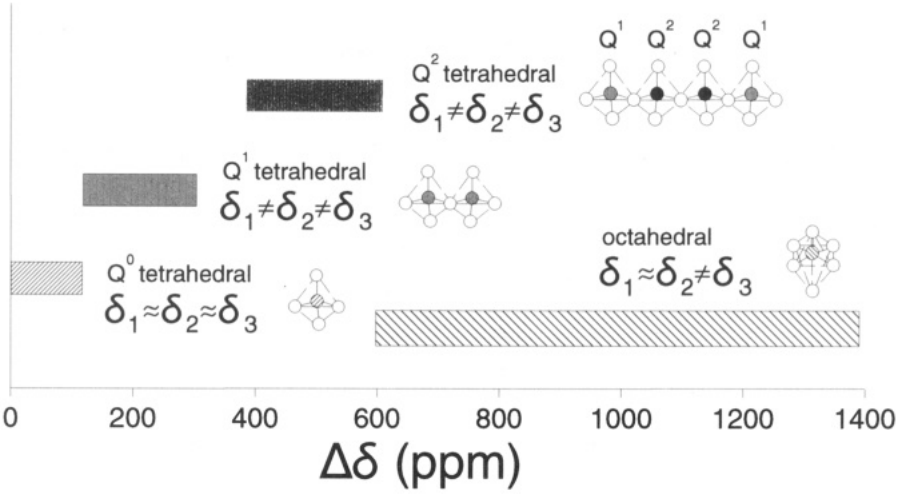

Figure 2. Width of the static ^{51}V chemical shielding anisotropy as a function of the vanadium coordination.

points: (a) Does the vanadium replace niobium by occupying the sites normally occupied by niobium in T-Nb_2O_5? (b) Does the number of neighboring vanadium atoms increase with increasing vanadium bulk concentration? (c) What is the chemical and structural environment of vanadium when present in the mixed phase β-$(Nb,V)_2O_5$ such that it is less active?

Solid-State NMR of the Quadrupolar Nucleus ^{51}V. The ^{51}V nucleus has had considerable attention in investigations using solid-state NMR, since this is a nucleus which is relatively easy to study because of its high natural abundance (99.76%), its high receptivity, and its rather small quadrupolar interaction. The small quadrupolar interaction results in spectra whose shapes are dominated by the chemical shift anisotropies. By comparing the line shapes with those of reference compounds of known structure, information on the oxygen coordination and the size of the vanadium-containing active site in a catalyst can be obtained. An excellent review of the application of ^{51}V solid-state NMR for the characterization of catalysts has been given by Lapina et al.,[13] while important pioneering work with V_2O_5 supported on Al_2O_3 and TiO_2 has been done by Eckert and Wachs.[14] A ^{51} solid-state NMR investigation of VO_x/Al−Nb−O catalysts was reported by de Oliveira et al.[15] Furthermore, a ^{51}V NMR study of V_2O_5/TiO_2 catalysts was recently published by Fernandez et al.[16]

From analysis of the static (i.e., nonspinning) line shapes of a large number of reference vanadates of known structures, Lapina et al.[13] have drawn a number of conclusions (see Figures 2 and 3, where Q^x is a tetrahedral site where x denotes the number of oxygen atoms shared between V species).

(a) For vanadium present in isolated tetrahedral sites (Q^0), chemical shift anisotropies of less than 100 ppm are found; for these sites, the V−O bond lengths are all equal, as are the values of the chemical shift tensor components δ_1, δ_2, and δ_3. (b) For vanadium present in slightly distorted tetrahedra which share one oxygen atom with a neighboring VO_4 tetrahedron (Q^1), asymmetric chemical shift tensors are found ($\delta_1 \neq \delta_2 \neq \delta_3$) which are typically between 100 and 300 ppm wide. (c) In strongly distorted vanadium tetrahedra which share two oxygen atoms with two different neighboring VO_4 tetrahedra (Q^2), vanadium gives an even larger and more asymmetric chemical shift anisotropy (400−600 ppm). (d) Vanadium can also be present in a distorted octahedral oxygen coordination with an axial symmetry; the NMR spectra of these compounds give very wide powder patterns (600−1400 ppm) with an axially symmetric chemical shift tensor ($\delta_1 \approx \delta_2 \neq \delta_3$). The isotropic chemical shift δ_{iso} has been found to be insensitive to the type of vanadium coordination. At the same time, for compounds

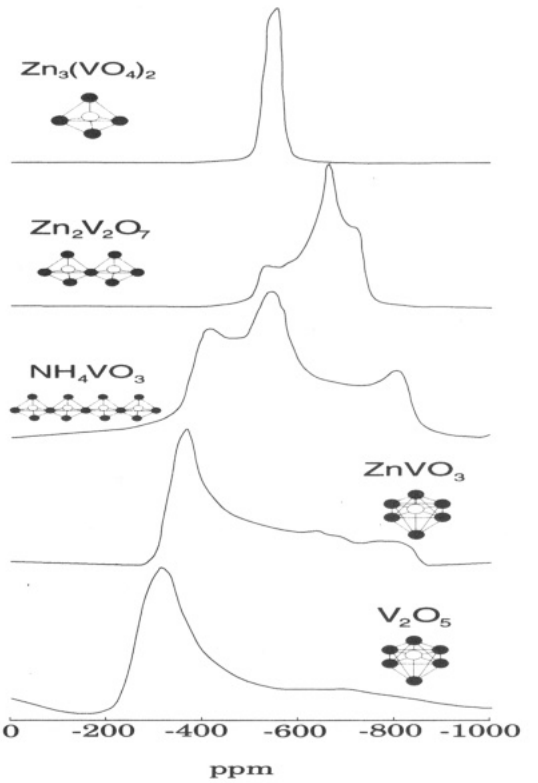

Figure 3. Static spectra of zinc orthovanadate (Q^0), zinc pyrovanadate (Q^1), ammonium metavanadate (Q^2), zinc metavanadate (distorted octahedral), and vanadium pentoxide (square pyramidal), demonstrating the strong dependence of the ^{51}V chemical shielding tensor on the coordination.

which show the same type of oxygen coordination, δ_{iso} has been found to be highly dependent on the type of atoms in the second coordination sphere (i.e., neighboring cations).

Eckert and Wachs[14] have found that the isotropic chemical shift may vary by as much as 22 ppm because of second-order quadrupolar effects when different field strengths of 7.1 and 11.7 T are used to carry out the experiments. This means that quadrupole coupling constants e^2qQ/h of up to 9 MHz are encountered. The size of this second-order quadrupolar shift is inversely proportional to the magnetic field and depends on the electric field gradient at the nucleus, this being proportional to the degree of distortion around the vanadium nucleus being studied.[17] It may thus provide additional information on the local environment of the nucleus. Accurate NMR analyses of a number of model compounds were performed by Skibsted et

al.[18] and Fernandez et al.[19] From spinning sideband analysis they obtained the chemical shift tensor, the quadrupole interaction, and their relative orientation.

Experimental Section

Sample Preparation. The coprecipitated catalyst samples described in this paper are the same as those described previously.[4,10] They are coded as V*x*Nb, where *x* is the intended mole percent of V_2O_5 in the Nb_2O_5.

Zinc vanadate reference samples were prepared by evaporation of solutions of $Zn(NO_3)_2{\cdot}4H_2O$ and NH_4VO_3 (Merck, p.a. quality) in the required ratios, followed by calcination in air at 630 °C for 5 h (ortho- and pyrovanadate) or 580 °C for 15 h (metavanadate). The orthovanadate ($Zn_3(VO_4)_2$) was found by XRD to be monophasic. The pyrovanadate ($Zn_2V_2O_7$) contained a trace of orthovanadate, and the metavanadate ($Zn(VO_3)_2$) contained some pyrovanadate. The reference samples of V_2O_5 (Merck No. 825) and NH_4VO_3 were used without further treatment.

Characterization. The experiments described in this paper were carried out at the SON HF-NMR Facility at the University of Nijmegen. Bruker CXP 300, AM 500, and AMX 600 spectrometers were used to carry out experiments at 7.05 T (79.0 MHz), 11.7 T (131.5 MHz), and 14.1 T (157.8 MHz), respectively.

Spectra were obtained with an excitation pulse of 1 μs duration, followed by a preacquisition delay of 4.5 μs. The delay between acquisitions was 2 s, which was sufficiently long to prevent any saturation effects.

The spectra were obtained using a home-built probehead equipped with a Doty 5 mm high-speed magic angle spinning assembly. To identify the isotropic chemical shifts, spectra were obtained at different spinning speeds using MAS frequencies up to 11 kHz.

Although an accurate quantitative evaluation of the spectra is desirable, this appeared to be not feasible for the spectra of the catalyst samples. Considering the complexity of the spectra, with strongly overlapping lines, very broad powder patterns and spinning sideband patterns, and thus large bandwidths, in combination with excitation effects that might influence the quantifiability of the spectra, we only analyzed them in a qualitative way. That is, the isotropic shifts and relative intensities of the lines were determined from the MAS spectra, and the total chemical shift anisotropy (CSA) was determined from the static spectra. Furthermore, these estimates of the CSA were verified by a spinning sideband analysis of the 14.1 T spectra using a PC program based on the Herzfeld and Berger method,[20] which is acceptable as these spectra are strongly dominated by the CSA whereas the influence of the quadrupolar interaction on the line shape is negligible at this field strength.

All chemical shifts reported here are given relative to that of liquid $VOCL_3$, using $Zn_3(VO_4)_2$ (isotropic line at −522 ppm, independent of field strength[14]) as the calibration standard. Considering the line width and the large bandwidth used to obtain the spectra, the accuracy of the peak positions is estimated to be 3 ppm.

Results and Interpretation of Spectra

Zinc Vanadates. The results of magic angle spinning (MAS) NMR of the zinc vanadates and V_2O_5 at the different field strengths are shown in Table 1, while the static spectra of these compounds and the NH_4VO_3 obtained are shown in Figure 3. The static spectra are typical powder patterns which become broader on going from zinc orthovanadate (Q^0 tetrahedral) to zinc pyrovanadate (Q^1 tetrahedral) and to ammonium metavanadate (Q^2 tetrahedral). The static spectra of zinc metavanadate, $ZnVO_3$, with distorted octahedral coordination and of vanadium pentoxide with square pyramidal or very distorted octahedral coordination show rather sharp peaks with long tails toward more negative ppm values. The valleys between the "peaks" are caused by the preacquisition delay of the instrument. This narrow peak shape in each case is explained by the axial symmetry around the vanadium nucleus ($\delta_1 = \delta_2$), while the length of the tail is proportional to the length of the longer V−O bond relative to the four equivalent shorter V−O bonds.[13]

TABLE 1: Results of MAS NMR of Zinc Vanadate Model Compounds and V_2O_5

sample	δ_{iso} (ppm) 7.1 T	11.7 T	14.1 T
$Zn_3(VO_4)_2$	−522	−522	−522
$Zn_2V_2O_7$	−622	−617	−617
$Zn(VO_3)_2$	−513	−501	−498
V_2O_5	−615	−614	−615

TABLE 2: Isotropic Shift Values and Width of the Static Lines for Vanadium Sites Occurring in the Catalysts Investigated

sample	δ_{iso} at 14.1 T (ppm)	$\Delta\delta$ (ppm)[f]	coordination[f]
V20Nb	−542	2000	dist oct
	−578[a]		tetr Q^1
	−602[b]		tetr Q^0
V15Nb	−578[a]	200	tetr Q^1
	−602[b]	<100	tetr Q^0
V10Nb	−578[a]	200	tetr Q^1
	−602	<100	tetr Q^0
V7.5Nb	−575[a]	200	tetr Q^1
	−602[b]	<100	tetr Q^0
	−630[c]	1000	dist oct
	−693[d]	small	tetr Q^1
V5Nb	−574[a]	200	tetr Q^1
	−602[b]	<100	tetr Q^0
	−630[c]	1200	dist oct
	−692[d]	small	tetr Q^1
V3Nb	−628[c]	1100	dist oct
	−694[d]	>100	tetr Q^1
	−713[e]	<100	tetr Q^0
V1.5Nb	−632[c]	1000	dist oct
	−695[d]	nd	tetr Q^1
	−715[e]	nd	tetr Q^0

[a] The accuracy of the determination of the isotropic shift is estimated to be 2−3 ppm, depending on the line width. In order to avoid confusion, we mention only one shift in the text; thus, this line is discussed as "the −578 ppm line" although for the different samples small (insignificant) changes are observed as is witnessed in this table. [b] Described as "the −602 ppm line" in the text. [c] Described as "the −630 ppm line" in the text. [d] Described as "the −693 ppm line" in the text. [e] Described as "the −713 ppm line" in the text. [f] nd, not determined; dist oct, distorted octahedral; tetr, tetrahedral.

The values of δ_{iso} (Table 1) found from the MAS spectra (not shown) for the zinc vanadates are in good agreement with those reported by Eckert and Wachs[14] and Lapina et al.[13] The value of δ_{iso} found here for V_2O_5 is somewhat more negative than that found by Eckert and Wachs[14] and by Lapina et al.[13] (−609 ppm).

Catalyst Samples. The MAS spectra of V20Nb, V10Nb, V7.5Nb, V5Nb, V3Nb, and V1.5Nb at 14.1 T are shown in Figures 4−9, respectively. Isotropic peaks are marked. The static magnitude spectra of V20Nb, V10Nb, and V7.5Nb are also displayed for each sample in the appropriate figure. The isotropic peak values at 14.1 T and the widths of the static lines at 14.1 T (estimated from the widths of the MAS spectra where no static spectra are available) of the different vanadium sites occurring in these materials are shown in Table 2. It should be noted that besides the strong spinning sidebands of the central

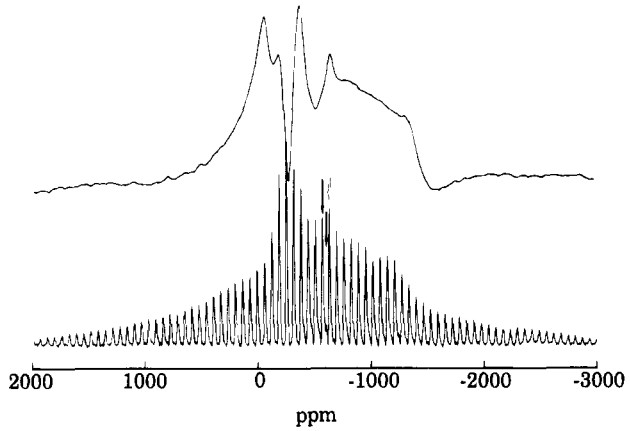

Figure 4. Static (top) and MAS (10.1 kHz, bottom) spectra of V20Nb at 14.1 T. Isotropic lines are indicated by filled arrows. Lines that were identified at different spinning speeds and field strengths but fall under a spinning sideband from another species in the present figure are indicated by open arrows.

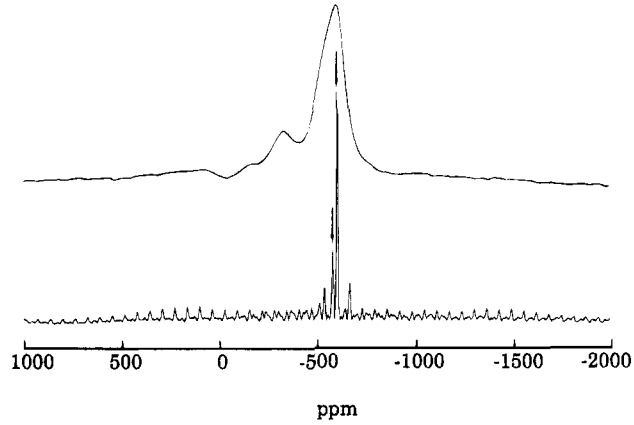

Figure 5. Static (top) and MAS (10.6 kHz, bottom) spectra of V10Nb at 14.1 T.

$-1/2 \rightarrow +1/2$ transition, weak spinning sidebands are observed covering the whole spectral range of the MAS spectra. These are due to partial excitation of transitions other than the central $-1/2 \rightarrow +1/2$ one and should not be included when estimating the chemical shift anisotropy.

The MAS and static spectra of V20Nb are shown in Figure 4; the former spectrum shows a large number of spinning sidebands and an isotropic peak at −542 ppm while the latter spectrum is approximately 2000 ppm wide, which is much broader than the spectra of any of the samples showing distorted octahedral vanadium sites reported by Eckert and Wachs[14] or Lapina et al.[13] As was discussed above, it is typical of octahedrally coordinated vanadium sites to have some axial symmetry ($\delta_1 \approx \delta_2 \neq \delta_3$). This is not the case here, however, since the principal tensor values are not equal to each other (δ_1 = +270 ppm, δ_2 = −330 ppm, and δ_3 = −1570 ppm as determined from the positions of the peaks and shoulders in the static spectrum). From this it can be concluded that the vanadium nucleus is likely to be a highly distorted octahedral coordination without any axial symmetry. Since the crystal structure of the main phase in this catalyst is not known, no correlation with the XRD results reported previously[4,10] can be given. A small proportion of other vanadium species with isotropic shifts at −578 and −602 ppm are also present. The latter signal is not visible in Figure 4 due to overlap with the spinning sidebands of the −542 ppm resonance, but it could be easily identified in spectra at different spinning speeds.

As shown in Figure 5, the V10Nb catalyst gave an entirely different MAS spectrum with a strong line at −602 ppm, which had only two spinning sidebands, and a smaller peak at −578 ppm, which had more small spinning sidebands. The feature at −620 ppm in the static spectrum can be interpreted as the combination of the narrow peak at −602 ppm and a broader peak overlapping this narrow peak. There is also a broad peak with a maximum at −317 ppm which can be attributed to an octahedrally coordinated species (see below, V7.5Nb). The spinning sidebands of this site are also visible in the MAS spectra, but due to heavy overlap and its low intensity we could not determine the isotropic chemical shift.

The isotropic peak at −602 ppm can be attributed to an isolated tetrahedral vanadium site (Q^0, see Figure 2) with a very small chemical shift anisotropy. The larger chemical shift anisotropy of the species giving the isotropic peak at −578 ppm suggests that this is a pyrovanadate-like tetrahedral site (Q^1). However, this is unlikely in view of the proposed crystal structure of β-$(Nb,V)_2O_5$; this will be discussed later. The two isotropic peaks at −602 and −578 ppm were also observed in the V15Nb sample and in other samples not reported here.[21] In all cases, they occurred simultaneously and in approximately the same intensity ratio; for these samples, β-$(Nb,V)_2O_5$ was also detected by XRD,[4] and so it is likely that these vanadium species occur in this phase. According to Goldschmidt,[22] β-$(Nb,V)_2O_5$ is structurally closely related to H-Nb_2O_5. This niobium oxide has blocks of niobium octahedra of two different sizes (3 × 5 and 3 × 4)[23] while one of the 28 Nb atoms in the unit cell is placed in one of the two tetrahedral positions occurring at the junctions of the blocks. These tetrahedral positions form chains in the *b*-direction of the unit cell but do not share edges or corners with each other. It was proposed by Wadsley and Anderson[11] that these niobium atoms are replaced by vanadium in β-$(Nb,V)_2O_5$. These vanadium atoms would then occur in isolated tetrahedral sites and give rise to the Q^0 sites observed at −602 ppm. In order to explain the occurrence of a Q^1 site (which seems the most likely for the line at −578 ppm, considering ^{51}V-NMR data published so far), one has to assume that both tetrahedral sites at the block junctions are occupied by vanadium in some cases. This is unlikely, however, as this would lead to unrealistically short V−V distances. Preliminary EXAFS results do not point to such short vanadium−vanadium distances. Another possibility which should be considered is that vanadium replaces niobium in the NbO_6 octahedra occurring in the blocks. A replacement of octahedrally surrounded Nb by Ti or W has been observed before.[11] If this replacement occurs for vanadium, the line at −578 ppm with a total anisotropy of only 200 ppm has to be attributed to octahedrally surrounded vanadium. This could be explained by the fact that the octahedra in the H-Nb_2O_5 structure are only slightly distorted. Although such a symmetric octahedral vanadium surrounding has not been reported before, it cannot be ruled out. It is clear that more work is necessary to get a definite assignment of this line.

The spectrum obtained for the V15Nb sample (not shown) showed the same two peaks as were found in the V10Nb sample, without the occurrence of the peak at −317 ppm in the static spectrum. In addition, a large number of small spinning sidebands occurred in the MAS spectrum, and these may be attributed to the unknown phase which occurred as the major phase in V20Nb.

Since the isotropic peaks at −602 and −578 ppm also occur in the MAS spectrum of the V7.5Nb sample (Figure 6), it can be concluded that this sample also contains some β-$(Nb,V)_2O_5$, although this is not the major phase. (This was confirmed by XRD.) The spectrum is dominated by a large number of

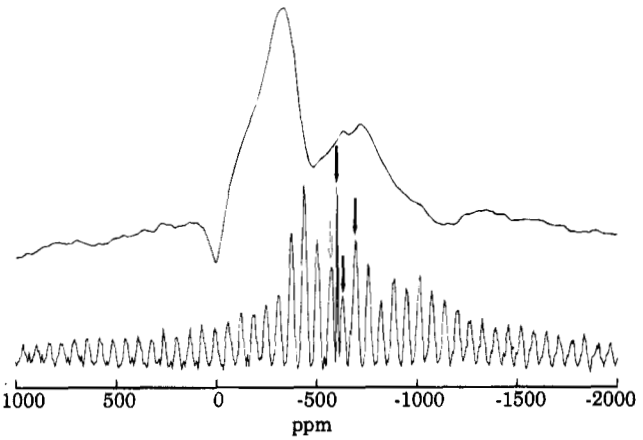

Figure 6. Static (top) and MAS (10.6 kHz, bottom) spectra of V7.5Nb at 14.1 T.

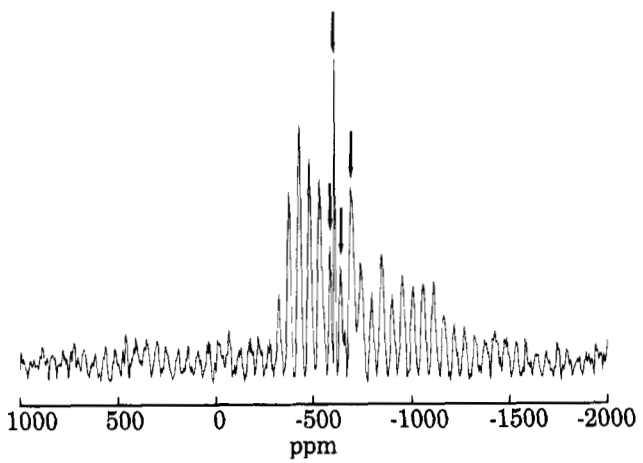

Figure 7. MAS (8.9 kHz spinning) spectrum of V5Nb at 14.1 T.

spinning side bands belonging to an isotropic peak at −630 ppm. At spinning speeds different from that used in Figure 6, a weak resonance of another vanadium species with an isotropic chemical shift of −693 ppm is found. The species responsible for the isotropic peak at −630 ppm is most likely a distorted octahedrally coordinated vanadium. The spinning sidebands belonging to this peak are much broader than the isotropic peaks at −578 and −602 ppm. A similar effect was also observed by Lapina et al. when studying vanadium catalysts.[14] These authors attribute this increased broadness to surface effects: the vanadium located at the surface of a catalyst (which may be a considerable part of the total amount of vanadium present) has a more heterogeneous environment than the vanadium located in the bulk of a crystal and thus gives broader peaks in a MAS spectrum. It is thus likely that the distorted octahedral species occur more at the surface while β-$(Nb,V)_2O_5$ occurs more in the bulk of the catalyst. The static spectrum can be interpreted as a combination of the static spectrum of the Q^0 species responsible for the isotropic peak at −602 ppm and that of the species having a distorted octahedral coordination which produces the isotropic line at −630 ppm in the MAS spectrum.

The MAS spectrum of the sample V5Nb (Figure 7) is similar to that of the sample V7.5Nb, except that the relative intensities of the various isotropic peaks have changed. The sizes of the −602 and −578 ppm peaks have become very small, and the size of the −693 ppm peak has increased with respect to the −630 ppm peak. The latter is still the dominant feature of the spectrum.

In the MAS spectrum of the sample V3Nb (Figure 8), the −630 ppm line is still dominant; the isotropic peak at −693

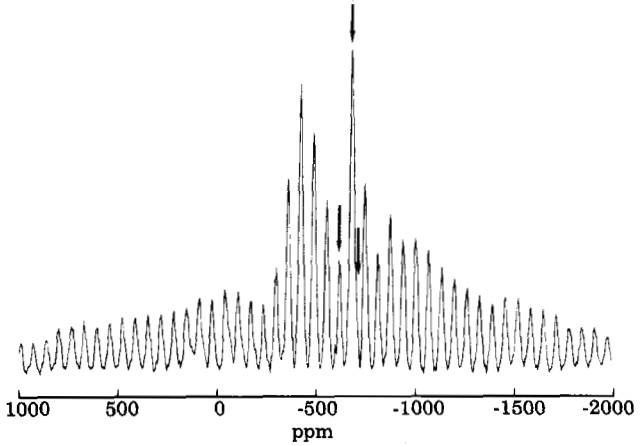

Figure 8. MAS (10.6 kHz) spectrum of V3Nb at 14.1 T.

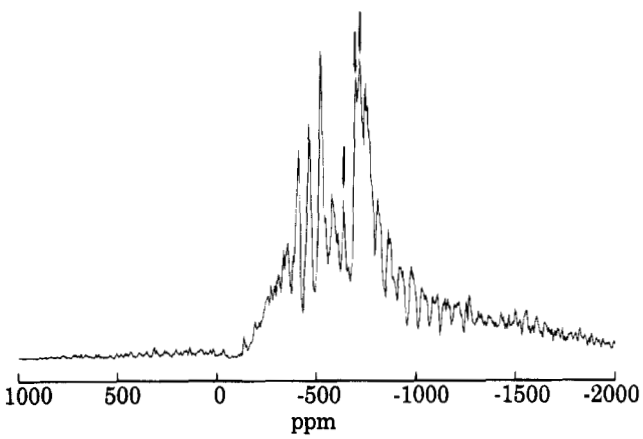

Figure 9. MAS (8.7 kHz) spectrum of V3Nb at 14.1 T.

ppm has become even clearer, however. The observation that this peak has a much greater intensity than the neighboring spinning sidebands means that this peak can be attributed to a rather symmetric vanadium species, possibly Q^1 or even Q^0. A new small isotropic peak occurs in this sample at −713 ppm, as a shoulder of the −693 ppm line.

The spectrum of sample V1.5Nb is presented as a MAS power spectrum, due to phasing problems (Figure 9). Many lines are visible: the −630, −693, and −713 ppm lines present in V3Nb and a series of broad overlapping lines in the −700 to −800 ppm range. The −713 ppm peak is more intense as compared to V3Nb. Note, however, that this is a power spectrum, and thus intensity differences are amplified. The species giving an isotropic peak at −693 ppm also gives a rather intense spinning sideband at −742 ppm, and this probably means that this species has a less symmetric vanadium environment than the species giving rise to the −713 ppm peak. It can thus be concluded that the species having an isotropic chemical shift of −713 ppm corresponds to an isolated tetrahedron, while the species having an isotropic chemical shift of −693 ppm has a Q^1 coordination symmetry. The various peaks in the −700 to −800 ppm range are not very well resolved from each other due to the superimposition of even broader lines. As was discussed above, this broadening can be attributed to the heterogeneity of the vanadium environment at the surface. It thus appears that such surface effects become more important as the vanadium concentration in the catalyst decreases.

The catalyst samples mentioned above were also investigated at a field strength of 11.7 T (131.5 MHz). No differences from the spectra described above were found, except for the fact that the quality of the spectra was not as good as those obtained at 14.1 T (157.8 MHz). No shifts in peak positions were observed

within experimental error, which indicates that second-order quadrupolar effects on the line positions are small. Calculations of the quadrupole induced shifts show that this means that the quadrupolar coupling constants are less than 5 MHz in all cases. Attempts to obtain well-resolved MAS spectra at 7.1 T, in order to gain more information concerning the quadrupolar interaction, failed due to second-order quadrupolar line-broadening effects.

Discussion

The results presented in this paper can now be correlated with the model for the catalysts which was summarized in the Introduction of this paper (Figure 1). In this model, it was assumed (a) that as the vanadium concentration in the catalyst increases, the number of vanadium atoms relative to niobium atoms in the second coordination sphere around the vanadium atom increases and (b) that this, in turn, causes the oxygen in the first coordination sphere to be more active.

The second of these assumptions was discussed[4,10,21] in relation to the work of Owen et al.,[24] who showed that the activity for the oxidative dehydrogenation of propane is inversely proportional to the reduction potential of the cation for a number of orthovanadates. It can thus be expected that a V−O−V ensemble is more active than a V−O−Nb ensemble because vanadium is more easily reduced than niobium.

The first assumption of the model is confirmed by the NMR results presented here. Up to a vanadium bulk concentration of 7 mol % V_2O_5, three different vanadium sites were detected in the catalysts: Q^0 and Q^1 tetrahedrally coordinated vanadium and distorted octahedral sites. Two observations can be made concerning these sites: (a) As the vanadium concentration increases, the intensity of the Q^1 coordinated vanadium site increases relative to that of the Q^0 sites (going from V1.5Nb to V3Nb), and the intensity of the distorted octahedral sites increases relative to that of the Q^1 sites (going from V3Nb to V7.5Nb). (b) A shift of the isotropic chemical shift is observed for the different coordinations, from −713 ppm for the Q^0 site to −693 ppm for the Q^1 site, and to −630 ppm for the octahedral site. The first observation confirms that as the amount of vanadium added to the catalyst is increased, the isolated vanadium sites initially formed at low concentration (Q^0 coordination) are transformed more and more into pyrovanadate-like sites (Q^1 coordination) by occupation of neighboring sites by vanadium. When the concentration of vanadium is increased further, these sites are replaced by octahedral sites. In most compounds in which vanadium occupies distorted octahedral sites, the octahedra also share oxygen atoms with neighboring octahedra (edge-sharing in many metavanadates, corner-sharing in decavanadates).

The second observation indicates that the number of neighboring niobium atoms decreases relative to the number of neighboring vanadium atoms on going from the Q^0 to octahedral coordination. Vanadium and niobium give different amounts of shielding to a vanadium nucleus when present in the second coordination sphere: niobium is less electronegative than vanadium and will thus draw less charge from the bridging oxygens. As was observed by Basler et al.,[25] vanadium shifts move toward more negative values (greater shielding) with decreasing electronegativity of its substituents. Thus, niobium in the second coordination sphere is thought to result in more shielding of the neighboring vanadium. If niobium is replaced by vanadium, the shielding is reduced and the isotropic peak of a site containing more vanadium in the second coordination sphere shifts to less negative ppm values. It should be noted, however, that the vanadium chemical shift is dominated by the paramagnetic term,[26] which critically depends on many factors, and thus some care should be taken in the interpretation of shift differences.

It was shown[4,10] that the T-Nb_2O_5 structure can accommodate approximately 7 mol % V_2O_5 without any change in the niobium oxide XRD pattern. It was suggested that vanadium replaces niobium in the crystal structure, possibly by occupying the sites which are normally occupied by niobium. The niobium ions in T-Nb_2O_5 are six-, seven-, or nine-coordinated with oxygen. The NMR spectra of these catalysts show distorted octahedral vanadium sites even at low concentrations of vanadium. This means that a large part of the vanadium can occupy the same sites as niobium in the catalyst. A small part of the vanadium appears to occupy the previously unfilled tetrahedral sites present in the undoped T-Nb_2O_5. Niobium vacancies are produced at the same time. It is likely that the positions occupied by the vanadium are more or less randomly distributed in the T-Nb_2O_5 since the addition of vanadium does not change the structure.

When β-$(Nb,V)_2O_5$ is formed, a very different niobium oxide structure is formed. Instead of the rather chaotic structure of T-Nb_2O_5, a very regular structure similar to that of the high-temperature H-Nb_2O_5 phase is formed. The vanadium is then forced to occupy one of the two isolated tetrahedral sites which are regularly spaced at the junctions of blocks of niobium octahedra. Sometimes both isolated tetrahedral sites are occupied, or vanadium occupies regular octahedral sites normally occupied by niobium.

Conclusions

From the results presented in this paper, it can be concluded that if the vanadium concentration in the catalyst samples is increased up to 7 mol % V_2O_5, most of the vanadium occupies the same sites as those normally occupied by niobium in T-Nb_2O_5, while a small part occupies tetrahedral sites. The relative number of tetrahedral sites is larger in samples containing less vanadium. As the vanadium concentration increases above a limit of approximately 7 mol % V_2O_5, isolated tetrahedral sites occur once again, and this can be ascribed to the formation of β-$(Nb,V)_2O_5$. In the unknown phase occurring in V20Nb, vanadium occupies distorted octahedral sites.

This model postulated on the basis of characterization of the catalysts using various techniques as well as from catalytic activity measurements appears to be consistent with the observations made with MAS-NMR in this study.

Acknowledgment. We thank G. H. Nachtegaal of the National HF-NMR Facility for invaluable experimental assistance. J. van Os and H. Janssen are thanked for their technical support. We thank the SON, The Netherlands, for the financial assistance to carry out this project.

References and Notes

(1) Seshan, K.; Swaan, H. M.; Smits, R. H. H.; van Ommen, J. G.; Ross, J. R. H. *Stud. Surf. Sci. Catal.* **1990**, *55*, 505.
(2) Haber, J. *Stud. Surf. Sci. Catal.* **1992**, *72*, 279.
(3) Roth, J. F. *Chem. Eng. News* **1993** (May 31), 27.
(4) Smits, R. H. H. Ph.D. Thesis, University of Twente, 1994.
(5) Smits, R. H. H.; Seshan, K.; Ross, J. R. H. *J. Chem. Soc., Chem. Commun.* **1991**, 558.
(6) Smits, R. H. H.; Seshan, K.; Ross, J. R. H. *Stud. Surf. Sci. Catal.* **1992**, *72*, 221.
(7) Smits, R. H. H.; Seshan, K.; Ross, J. R. H. In *Catalytic Selective Oxidation*; Oyama, S. T., Hightower, J. W., Eds.; ACS Symposium Series No. 523; American Chemical Society: Washington, DC, 1992; p 380.
(8) Ross, J. R. H.; Smits, R. H. H.; Seshan, K. *Catal. Today* **1993**, *16*, 503.
(9) Smits, R. H. H.; Seshan, K.; Leemreize, H.; Ross, J. R. H. *Catal. Today* **1993**, *16*, 513.

(10) Smits, R. H. H.; Van den Oetelaar, L. C. A.; Seshan, K.; Anantharaman M. R.; Brongersma, H. H.; Ross, J. R. H. *J. Catal.*, submitted.

(11) Wadsley, A. D.; Anderson, S. In *Perspectives in Structural Chemistry*; Dunitz, J. D., Ibers, J. A., Eds.; John Wiley & Sons: New York, 1990; Vol. 3, p 19.

(12) Kato, K.; Tamura, S. *Acta Crystallogr.* **1975**, *B31*, 673.

(13) Lapina, O. R.; Mastikhin, V. M.; Shubin, A. A.; Krasilinikov, V. N.; Zamaraev, K. I. *Prog. NMR Spectrosc.* **1992**, *24*, 457.

(14) Eckert, H.; Wachs, I. E. *J. Phys. Chem.* **1989**, *93*, 6796.

(15) Pries de Oliveira, P. G.; Lefebre, F.; Eon, J. G.; Volta, J. C. *J. Chem. Soc., Chem. Commun.* **1990**, 1480.

(16) Fernandez, C.; Bodart, Ph.; Guelton, M.; Rigole, M.; Lefebvre, F. *Catal. Today* **1994**, *20*, 77.

(17) Freude, D.; Haase, J. In *NMR Basic Principles and Progress*; Diehl, E., Fluck, E., Günther, H., Kosfeld, R., Selig, J., Eds.; Springer-Verlag: Berlin, 1993; Vol. 29, pp 1−90.

(18) (a) Skibsted, J.; Nielsen, N. Chr.; Bildsøe, H.; Jakobsen, H. J. *Chem. Phys. Lett.* **1992**, *188*, 405. (b) *J. Am. Chem. Soc.* **1993**, *115*, 7351.

(19) Fernandez, C.; Bodart, P.; Amoureux, J. P.; *Solid-State Nucl. Magn. Reson.* **1994**, *3*, 79.

(20) Herzfeld, J.; Berger, A. E. *J. Chem. Phys.* **1980**, *73*, 6021.

(21) (a) Smits, R. H. H.; De Vries, Y. A.; Seshan, K.; Ross, J. R. H. *Proc. 2nd Tokyo Conf. Adv. Catal. Sci. Technol., Tokyo, Aug 21−26, 1994.* (b) *Stud. Surf. Sci. Catal.*, in press.

(22) Goldschmidt, H. J. *Metallurgia* **1960**, *62*, 211.

(23) Gatehouse, B. M.; Wadsley, A. D. *Acta Crystallogr.* **1964**, *17*, 1545.

(24) Owen, O. S.; Kung, M. C.; Kung, H. H. *Catal. Lett.* **1992**, *12*, 45.

(25) Basler, W.; Lechert, H.; Paulsen, K.; Rehder, D. *J. Magn. Reson.* **1981**, *45*, 170.

(26) Rehder, D. In *Multinuclear NMR*; Mason, J., Ed.; Plenum Press: New York, 1987; Chapter 19.

JP943036K